Computational and Structural Biotechnology Journal 19 (2021) 2460–2467

COMPUTATIONAL AND STRUCTURAL BIOTECHNOLOGY JOURNAL

journal homepage: www.elsevier.com/locate/csbj

Structural characterization of PaFkbA: A periplasmic chaperone from *Pseudomonas aeruginosa*

Qin Huang [1], Jing Yang [1], Changcheng Li, Yingjie Song, Yibo Zhu, Ninglin Zhao, Xingyu Mou, Xinyue Tang, Guihua Luo, Aiping Tong, Bo Sun, Hong Tang, Hong Li, Lang Bai *, Rui Bao *

Center of Infectious Diseases, State Key Laboratory of Biotherapy, West China Hospital, Sichuan University and Collaborative Innovation Center, Chengdu, China

ARTICLE INFO

Article history:
Received 19 November 2020
Received in revised form 19 April 2021
Accepted 22 April 2021
Available online 25 April 2021

Keywords:
FKBP-type protein
Chaperone activity
Crystal structure
Inter-domain rearrangement
Pseudomonas aeruginosa

ABSTRACT

Bacterial Mip-like FK506-binding proteins (FKBPs) mostly exhibit peptidyl–prolyl-cis/*trans*-isomerase (PPIase) and chaperone activities. These activities are associated with various intracellular functions with diverse molecular mechanisms. Herein, we report the *PA3262* gene-encoded crystal structure of the *Pseudomonas aeruginosa* PAO1's Mip-like protein PaFkbA. Biochemical characterization of PaFkbA demonstrated PaFkbA's chaperone activity for periplasmic protein MucD, a negative regulator of alginate biosynthesis. Furthermore, structural analysis of PaFkbA was used to describe the key features of PaFkbA chaperone activity. The outcomes of this analysis showed that the hinge region in the connecting helix of PaFbkA leads to the crucial conformational state transition for PaFkbA activity. Besides, the N-terminal domains participated in dimerization, and revealed its potential connection with FKBP domain and substrate binding. Mutagenesis and chaperone activity assay supported the theory that inter-domain motions are essential for PaFkbA function. These results provide biochemical and structural insights into the mechanism for FKBP's chaperone activity and establish a plausible correlation between PaFkbA and *P. aeruginosa* MucD.

1. Introduction

FK506-binding proteins (FKBPs), the member of immunophilin family, are characterized by a cis–trans peptidyl-prolyl isomerase (PPIase) and chaperone activity [1,2]. FKBPs is a co-receptor for the natural products FK506 and rapamycin. Besides, it is widely distributed in prokaryotic and eukaryotic cells. FKBPs are involved in multiple celluar functions, such as protein folding, assembly, trafficking, function regulation, and various signaling pathways [1,3]. In bacteria, virulence-related FKBP-type PPIase MIP (macrophage infectivity potentiator) was first identified in *Legionella pneumophila* [4,5], after which Mip-like FKBPs have been continuously discovered in different species and their potential functions in pathogenesis were investigated [6].

L. pneumophila Mip (LpMip) is a cell-surface protein, which is functionally similar to adhesin, it facilitates attachment on lung epithelial cells with collagen IV [7]. Apart from transporting bacterial cells across an epithelial cell barrier, LpMip plays a crucial role in *L. pneumophila* motility, environmental stress adaptation, and type II secretion system [8,9]. Mip-like PPIases from multiple pathogenic bacteria and protozoan parasites, such as *Coxiella burnetii* [10], *Burkholderia pseudomallei* [11], *Neisseria gonorrhoeae* [12], *Chlamydia psittaci* [13], *Trypanosoma cruzi* [14], and *Leishmania infantum* [15] have cell location and biological properties similar to that of LpMip. Although Mip-like proteins are not secreted to the cellular surface in certain pathogens, *Mip*-like genes are essentially required for the full virulence of these pathogens [16]. Mip homologs, FkpA and FklB (also named as FKBP22), in periplasm and cytoplasm of *Escherichia coli* have been implicated to be essential for various cellular processes such as cell motility, biofilm formation, outer-membrane protein biogenesis, EspP autotransporter function, and bactericidal colicin M uptake [17–19]. Therefore, Mip-like FKBP, which regulates microbe-associated diseases, is treated as a potential therapeutic target in the drug development studies.

Previous structural studies on Mip and its homologs have revealed a conserved V-shape dimeric assembly in MIP. In this dimeric assembly each monomer is divided into three major parts: an N-terminal dimerization module, a hinge region in connecting α-helix, and a C-terminal FKBP domain [20,21]. FKBP domain's

* Corresponding authors.
E-mail addresses: pangbailang@163.com (L. Bai), baorui@scu.edu.cn (R. Bao).
[1] These authors contributed equally.

https://doi.org/10.1016/j.csbj.2021.04.045

biochemical analysis discern its peptidyl-prolyl isomerase mechanism and binding pattern with the FK506 ligand [20–22]. In particular, the hinge-related domain motions and N-terminal-mediated dimerization rely on Mip's internal molecular interactions. Previous studies suggest that domain motions regulate the chaperone activity of Mip-like FKBPs [23–26]. Rolf Kohler et al. showed that LpMip$^{(77\text{-}213)}$ in monomeric fragment had a notably reduced chaperone activity for RCM-T_1 folding, while Kaifeng Hu et al. addressed the importance of the FKBP domain in the initiation of protein binding [24–26]. These studies demonstrated the role of different modules in the protein folding pathway. However, further in-depth investigations are required to explore the impacts of the domain association on Mip-like FKBPs function to better understand the correlation between its structure and chaperone activity.

In the opportunistic pathogen *Pseudomonas aeruginosa*, *PA3262* gene-encoded Mip-like protein was predicted to contain a lipoprotein sorting signature for inner membrane localization [27]. Previous studies have associated Mip-like protein with bacterial cell envelope secreted by outer membrane vesicles (OMVs) [28,29]. Due to the high sequence identity (39.4%) with *E. coli* FkpA (EcFkpA), in this study, we denote the Mip-like protein as PaFkbA. Proteomic analysis of PaFkbA revealed that it is involved in adapting the *P. aeruginosa* cells to the cystic fibrosis (CF) lung microenvironment [30]. However, literature related to the PaFkbA function is minimal, and its underlying molecular mechanism remains elusive.

In this study, we have shown that PaFkbA could mediate the in vitro refolding of the periplasmic protein MucD, a negative regulator of alginate production in *P. aeruginosa* [31]. The outcomes of structural and biochemical analyses of MucD demonstrated that chaperone activity of MucD is dependent on its N- and C-terminal domains. Moreover, different PaFkbA conformations in crystal structure validated the importance of connecting α-helix for inter-domain rearrangements. Site-directed mutagenesis studies unveiled that the inter-domain association is vital for the full function of PaFkbA. The structural and biochemical characterization of PaFkbA provided experimental evidence for the role of the dynamic inter-domain movement in Mip-like FKBP function and demonstrated the chaperone activity of PaFkbA for MucD.

2. Materials and methods

2.1. Bacterial strains and medium

Escherichia coli BL21(DE3), *Escherichia coli* DH5α and *Pseudomonas aeruginosa* PAO1 (from the laboratory collection) were used in this study. All *E. coli* strains were grown in Luria broth (LB) with 50 μg/mL ampicillin sodium. For preparation of genome DNA, a single colony of *P. aeruginosa* PAO1 was cultured in LB medium overnight in presence of 26 μg/mL irgasan at 37℃.

2.2. Protein expression and purification

The gene *fkbA* (Uniprot code Q9HYX8) and *mucD* (Uniprot code G3XD20) were amplified from the *P. aeruginosa* genomic DNA by polymerase chain reaction (PCR) and inserted into pET22b plasmid between the start codon site and His6-tag by ClonExpress® MultiS One Step Cloning Kit (Vazyme). For crystallization, *PA3262* was attached with a C-terminal sequence specificity of TEV protease. Site-specific mutants were constructed by Blunting Kination Ligation (BKL) Kit (Takara). All primers were shown in Table A1. These constructs were confirmed by sequencing. All proteins were produced in *E. coli* strain BL21(DE3) and purified by a similar method. Briefly, cells were cultured in LB medium in presence of ampicillin at 37℃ to an OD_{600nm} of 0.8 and induced with 0.4 mM Isopropyl-beta-D-thiogalactopyranoside (IPTG) for 16 h at 16 °C. Cells were lysed by sonication in buffer A (25 mM Tris-HCl, pH 7.5, 150 mM NaCl) and lysates were centrifuged for 30 min at 18,000 rpm to remove insoluble materials. The supernatant was loaded onto Ni–NTA resin (Qiagen) preequilibrated with buffer A, then washed with buffer B (buffer A containing 30 mM imidazole). The protein was eluted with buffer C (buffer A added with 300 mM imidazole), further concentrated and purified by anion-exchange chromatography and gel chromatography on an ENrich SEC 650 column (Bio-rad). Peak fractions were analyzed by SDS-PAGE and stored at −80℃.

2.3. Crystallization, data collection and structure determination

For crystallization, the His6 tagged PaFkbA-Δc (residues 23–228, lacking the C-terminal residues of 229–253), purified in buffer D (25 mM HEPES, pH 7.5, 150 mM NaCl) via a similar way, was overnight treated with TEV protease at 4 °C and loaded onto Ni–NTA resin before anion-exchange chromatography. Purified protein PaFkbA-Δc was concentrated to 13 mg/mL and crystallized by a sitting-drop vapor diffusion method at 16 °C. Initial crystals were grown in several reservoir solutions, after optimization, the high-quality crystals of PaFkbA-Δc were obtained under conditions of 0.1 M Tris (pH 8.0), 28% PEG4000 in 3–4 days. Single crystal was rapidly swept through reservoir solutions containing PEG400 as a cryoprotectant and flash-cooled in liquid nitrogen. X-ray diffraction data was collected at National Center for Protein Sciences Shanghai (NCPSS) beamlines BL18U.

All diffraction intensities were integrated and scaled by the HKL2000 software package [32]. The data were processed to a resolution of 2.9 Å in space group $P2_12_12_1$ with unit cell parameters of a = 77.07 Å, b = 94.22 Å, c = 117.44 Å. The phase problem was solved by using Phaser-MR (full-featured) as implemented in PHENIX with the PPIase domain of EcFkpA (PDB code 1q6u, 39.4% sequence identity) as a template [33]. The process of structure building and refinement was monitored using PHENIX and Coot [34]. Meanwhile, the torsion-angle-based NCS restraints was implemented in refinement process. The figures were prepared by using The PyMOL Molecular Graphics System [35].

2.4. MucD proteolytic activity assay

An internally quenched fluorescent peptide substrate (Abz)-TVAW-pNA was commercially synthesized (ALL PEPTIDE). This quenched fluorescence is liberated upon the cleavage of peptide by MucD, resulting in increased fluorescence that could be monitored fluorometrically. MucD (at a final concentration of 7 mg/mL) was denatured using 10 M urea for 1 h, followed by diluting urea to 0.25 M with buffer A containing 1 mM DTT and PaFkbA-Δc (at varying concentration) for 30 min at 16 ℃. In the control group, chaperone-free buffer A was added for renaturation. The chaperone activity of PaFkbA-Δc was tested using a relative proteolytic activity of refolded MucD (chaperone or buffer A treated MucD). Proteolysis system included 40 μL buffer A, 50 μL refolded MucD, and 10 μL substrate (dissolved in 50% DMSO, at a concentration of 500 μM). Relative Fluorescence Unit was monitored using a microplate reader at 310 nm for excitation and 420 nm for emission. Chaperone activity of PaFkbA-Δc was reflected by mucD proteolytic cleavage rates. The activities of other mutants were measured with a same method above.

2.5. Statistical analyses

Statistical analyses were performed with GraphPad Prism, and P values for the differences between means were determined by the

one-way analysis of variance (ANOVA) statistical test with equal variances. Results were considered significant if the *P* value was 0.05 < (*), 0.01 < (**), 0.001 < (***), or 0.0001 < (****).

3. Results

3.1. Chaperone activity of PaFkbA towards the HtrA-like protease MucD

In gram-negative bacteria, a porous outer membrane separates periplasm from the external environment. Thus, the periplasmic proteins are more readily exposed to stress conditions than their cytoplasmic counterparts, increasing the protein's unfolding and folding events in the periplasm[36]. Periplasmic chaperones prevent the aggregation of the newly synthesized or stress-denatured proteins [37,38]. The periplasmic FkbA protein EcFkpA from *E. coli* possesses intrinsic chaperone activity and interplay with DegP which is also a periplasmic chaperone belonging to HtrA-type *endo*-serine protease family [17,21], implying that a cooperative refolding mechanism of different chaperones may contribute to the efficient protein refolding process [38–41]. In *P. aeruginosa*, MucD, which is involved in alginate synthesis, is a DegP homolog and, it may have a functional resemblance with PaFkbA [42,43]. For biochemical assessment of the plausible interaction between PaFkbA and MucD, we designed an in vitro PaFkbA chaperone activity assay using unfolded MucD as substrate. Purified MucD was denatured using urea and subsequently refolded in solution with or without PaFkbA (molar ratios of MucD to PaFkbA: 1: 1, 1: 5, 1: 10). Later, the proteolytic activity of refolded MucD was detected using synthesized fluorescent substrate (Abz)-TVAW-pNA [44].

The soluble and matured form of PaFkbA (23–253) without the predicted N-terminal signal peptide was expressed and purified in *E. coli* BL21[22]. Twenty-five residues at C-terminal tail were predicted to be flexible, which made them inapt for crystallization, thus, we prepared the truncated form of PaFkbA-Δc (23–228). The fluorescent substrate cleavage data showed that the PaFkbA-Δc increased the MucD refolding in a dose-dependent manner (Fig. 1A, Figure A1). Meanwhile, PaFkbA couldn't refold two urea-denatured serine proteases, algW and trysin (Figure A2). It suggested that PaFkbA served as a chaperone to maintain MucD activity in vitro. Interestingly, PaFkbA-Δc exhibited 2.2-fold higher chaperone activity than PaFkbA (Fig. 1B). It indicated that the C-terminal flexibility might affect the PaFkbA's chaperone activity. Lack of the disorder C-terminal tail seems dispensable for the activity. It is in line with the chaperon activity of other FKBP-like PPIase, such as EcSlyD, which has several Ni^{2+} binding sites in the C-terminal tail [45]. Thus, the PaFkbA tail interaction with a macromolecular partner may confer stability to PaFkbA, which could be used to regulate PaFkbA's activity in vivo.

3.2. Overall structure of PaFkbA

In this study, both PaFkbA and PaFkbA-Δc were used for crystallization trials. We obtained the PaFkbA-Δc crystal and solved its crystal structure at 2.9 Å resolution in space group $P2_12_12_1$. Residues 25–228 were modeled into the electron density, which resulted in a final model with R_{free} of 0.281 and R_{work} of 0.245. The detailed crystallographic and refinement statistics are shown in Table 1.

The asymmetric unit entails four molecules (chain A/D/F/G) with two cradle-shaped dimers (Fig. 2A). In line with other Mip-like proteins [20,21], each PaFkbA-Δc monomer could be divided into distinct functional modules. The N-terminal dimerization domain (residues 25–69) consists of two short α-helices, α1 (residues 31–47) and α2 (residues 57–69), entwining with the N-domain helices of the adjacent monomer. The N-terminal domain provides all inter-chain interactions by forming a non-canonical anti-parallel four-helix bundle. The C-terminal FKBP domain (residues 120–227), which belongs to the typical FKBP fold, was characterized by an anti-parallel six-stranded β-sheet flanked by a short α-helix α4 (residues 178–186). FKBP domain is responsible for FK506 binding and PPIase activity. Besides, the FKBP domain catalyzes the interconversion of prolyl cis/trans conformation facilitating the correct folding of certain proteins [46]. The surface representation of the FKBP domain demonstrates a substrate-binding cavity with a surface area of 484.8 $Å^2$. This cavity facilitates the peptidyl-prolyl substrate binding within these regions (Fig. 2B). FKBP and dimerization domains are connected through oppositely placed long α-helix α3 (residues 77–115). In one of the PaFkbA-Δc dimers, the connecting α3 from non-equivalent monomers exhibits distinct orientations, resulting in monomers with different inter-domain angles of 129.7° and 26.86° (Fig. 2C). It indicates independent inter-domain motion within the PaFkbA dimer. The plausible mechanism for Mip-like FKBPs binding to large substrate proteins might involve different distances between the FKBP domain and the dimerization domain, as per the previous studies [23,26].

3.3. The functional domains of PaFkbA exhibit distinct conservation patterns

Multiple structural studies have been carried out on Mip-like proteins from *E. coli*, *L. pneumophila*, and *Shewanella* spp. SIB1 [20,21,25], and only near-full-length structures of EcFkpA (PDB code 1q6u, 39.4% sequence identity to PaFkbA) and LpMip (PDB code 1fd9, 41.3% sequence identity to PaFkbA) are available. The flexible connecting α-helix resulted in high RMSD values (3.19–2.74 Å) for LpMip, EcFkpA, and PaFkbA in an overall structure (25–228 aa) superposition (Fig. 2D). However, their functional modules exhibited high structural similarity. The individual domain superposition for the FKBP domain (120–227 aa) and dimerization domain (25–69 aa) had an average RMSD value of 0.89 Å and 1.6 Å, respectively.

FKBP domain is a highly conserved motif, which is found in numerous species. Despite sharing a high degree of structural similarity with the PPIase fold, multiple FKBP domains are inactive as the PPIase activity essentially relies on the integrity of active site residues [47]. In human FKPB12, numerous hydrophobic, specifically aromatic residues (Y27, F37, F47, F49, V56, I57, W60, Y83, I92, and F100) constitute the half β barrel shaped active site cavity, which is flanked by several charged residues (D38, R43, E55, and H88). The key active-site residues for PPIase activity are central hydrophobic and D38 residues [47]. The vital role of these sites in FK506 binding was validated in LpMip and EcFkpA [20,21]. The outcomes of sequence alignment showed that important residues were 100% conserved in Mip-like FKBPs except for the positions corresponding to the F47 and F49 in HuFKPB12, where the Phe residues were replaced by I169 and L171 in PaFkbA (Fig. 3). Based on the FK506-complexed EcFkpA structure (PDB code 1q6i) [21], we constructed an FK506-PaFkbA binding model by superimposing the FKBP domains (Fig. 4A). We observed that FK506 was well-fitted into the hydrophobic pocket and interacted extensively with the equivalent functional hydrophobic residues of PaFkbA. The pipecolinyl ring that mimics a peptidyl-prolyl bond was in close proximity to W180, Y149, F220, and Y203 residues. Substitutions of Phe residues with smaller hydrophobic I169 and L171 did not introduce any steric clash, but it enhanced the accessibility for

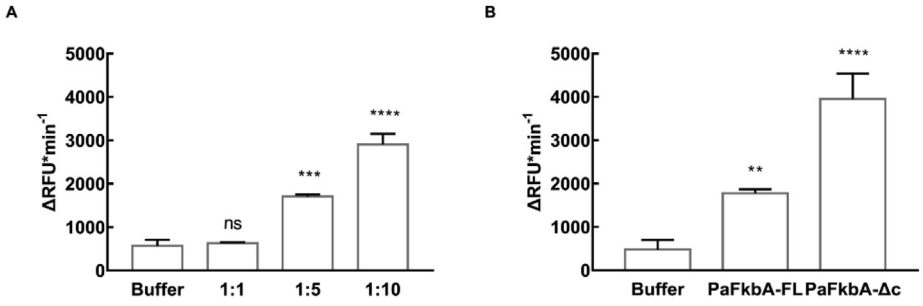

Fig. 1. Proteolytical assay of refolded MucD. **A.** Molar ratios between MucD and PaFkbA-Δc. B. Comparing the chaperone activities of full length PaFkbA (PaFkbA-FL) and PaFkbA-Δc. Molar ratio (MucD: PaFkbA) used was 1:10. Error bars represent the standard deviation of three duplicate trials. Statistical significance was calculated by one-way ANOVA (*, P < 0.05; **, P < 0.01; ***, P < 0.001, ****, P < 0.0001; ns, not significant).

Table 1
Statistics on the qualities of diffraction data and model refinement.

Data Collection	Wavelength (Å)	0.97853
	Space group	$P2_12_12_1$
	Cell dimensions	
	a, *b*, *c* (Å)	77.07 94.22 117.44
	Resolution (Å)[a]	40.00–2.90 (3.00–2.90)
	No. of unique reflections	19,438 (1904)
	CC (1/2)	0.99 (0.69)
	R_{merge} (%)[b]	9.9 (47.2)
	I/σ (*I*)	48.8 (2.15)
	Completeness (%)	99.8 (99.7)
	Redundancy	8.6 (6.2)
	R_{pim} (%)[c]	1.7 (20.1)
Refinement	Wilson B-factor (Å^2)	68.5
	R_{work}/R_{free} (%)[d]	24.5/28.1
	B-factors (Å^2)	
	Protein (global)	84.4
	Water	66.5
	No. atoms	6195
	Protein	6138
	Water	57
	R.m.s deviations	
	Bond lengths (Å)	0.012
	Bond angles (°)	1.59
	Ramachandran plot (%)	
	Total favored	96.28
	Total allowed	3.22
	Total outliers[e]	0.5

[a] The number in parentheses is for the outer shell.
[b] $R_{merge} = \sum_{hkl}\sum_i |I_i(hkl) - <I(hkl)>| / \sum_{hkl}\sum_i I_i(hkl)$, where $I_i(hkl)$ is the intensity measured for the *i*th reflection and $<I(hkl)>$ is the average intensity of all reflections with indices hkl.
[c] $R_{pim} = \sum_{hkl} [1/(N-1)]^{1/2} \sum_i |I_i(hkl) - <I(hkl)>| / \sum_{hkl}\sum_i I_i(hkl)$.
[d] $R_{work} = \sum_{hkl} | |F_{obs}(hkl)| - |F_{calc}(hkl)| | / \sum_{hkl} |F_{obs}(hkl)|$; R_{free} is calculated in an identical manner using 10% data excluded from refinement.
[e] Four outliers were found around A202 in chain A/D/F/G, as shown in Figure A3.

FK506. Thus, the extensive conservation of the active site residues indicates that the PPIase activity is a common feature in Mip orthologs.

In contrast to the widely distributed and highly conserved FKBP domain, the N-terminal dimerization domain and the connecting α3 are present only in Mip-like FKBPs, displayed low sequence similarities (Fig. 3). Dimerization is essential for the function of Mip-type FKBP [24]. Thus, the residues essential for the dimer associations are relatively conserved, especially the two pairs of hydrophobic "zipper knot" residues, I39/M43 and V60/I64 (Figs. 3 and 4B). These residues are involved in the primary mechanism for the symmetric inter-chain contacts between the anti-parallel helices. Similarly, in the α3 region, a hydrophobic patch, F109 and V119 in PaFkbA (Fig. 4B) that mediates the interaction with the FKBP domain also displays high conservation (Fig. 3). Overall, these conserved structural elements ensure a common scaffold, reflecting a unique accessory function of the N-terminal domains.

3.4. The hinge region at α3 is essential for the inter-domain arrangement

NMR spectroscopy and molecular dynamics (MD) simulation studies on LpMip have identified the independent interdomain motions and speculated that it might be crucial for LpMip to act as a clip during substrate recognition [23]. Similar domain flexibility was also observed when the LpMip with EcFkpA were compared. These structural variations might result from the dynamic structural adaption of the connecting α3. Besides, they might be involved in controlling the cleft region's shape to accommodate the unfolded protein substrate and provide an additional layer of control to the prolyl isomerization of FKBP domains [21]. LpMip and EcFkpA structures available so far reveal a set of closely related "open" conformation where the cleft is exposed to the solvent [20,21]. However, as mentioned above, the two PaFkbA monomers within one dimer were folded into two different conformational states. The cleft of one PaFkbA monomer (average B-factor of main chain: 92.5 Å^2) showed an approximate width of 26.2 Å (distance of C-alphas from E78 to R165), whereas another monomer (average B-factor of main chain: 83.5 Å^2) displayed a much smaller cleft of approximately 8.2 Å. Thus, PaFkbA monomer with a smaller cleft is more likely to represent a "closed" state due to a narrower cleft region occluding the entrance by the N-terminal dimerization domain from the neighboring monomer (Fig. 5A). Furthermore, examination of the closed conformation revealed some "charge patches" (N42, K45, Q73, E164 and R165 from chain G; D77 and E78 from chain A), involved in mediating the compact domain organization (Fig. 5B), containing the residues facing the hydrophobic cavity on N-terminal half of the cleft. It suggested that domain closure might be linked to the substrate-binding mechanism.

The conformational transitions discussed above indicated that the structural feature of α3 may affect the enzymatic efficiency and mechanism of the PaFkbA. The structural determinants responsible for the domain mobility were traced by superposing the dimerization domains of "open" and "closed" PaFkbA structures. We observed that a positive charge region (R90 and R94) was located at the middle of α3 and a negative charge cluster (D53 and D54) at the turn between α1 and α2 (Fig. 5C). Thus, we hypothesized that the formation and disassociation of the ionic interactions between these two opposing charged surfaces might be associated with the transition of the "closed"-"open" states. Accessory domain in multi-domain PPIases serves as a scaffold for complex formation and regulates PPIase domain activity [48,49]. The molecular interactions at the α3 hinge may serve as

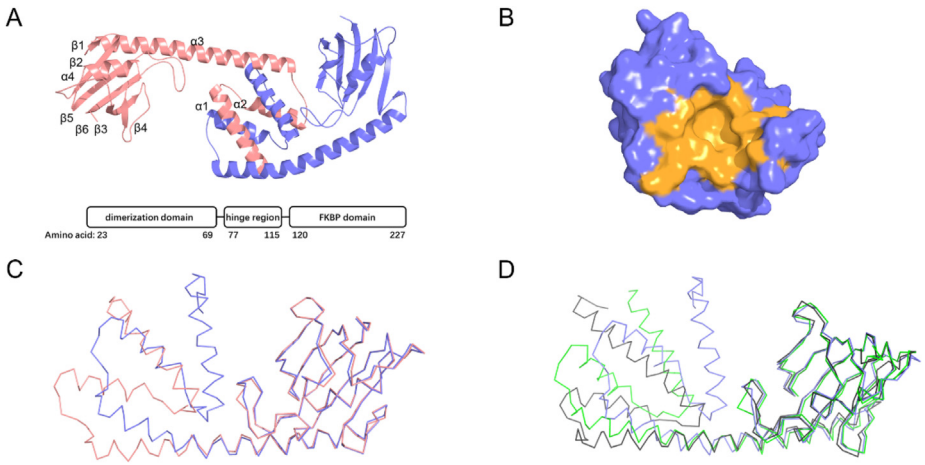

Fig. 2. Schematic representation of the crystal structure of the PaFkbA-Δc. A. The overall structure in cartoon representation. One monomer is colored in blue (chain A) and the other is in pink (chain G). The secondary structural elements including six β-sheets and four α-helices are labeled. B. PaFkbA-Δc FKBP domain in surface representation, where the yellow region indicates the conserved FK506-binding pocket. The Accessible Surface areas suite in CCP4Interface was used. C. Structural comparison of Chain A and Chain G using the FKBP domain as an anchor point. It was calculated with structural analysis suite in Chimera. D. Superpose of PaFkbA (blue), EcFkpA (black) and LpMip (green). (For interpretation of the references to colour in this figure legend, the reader is referred to the web version of this article.)

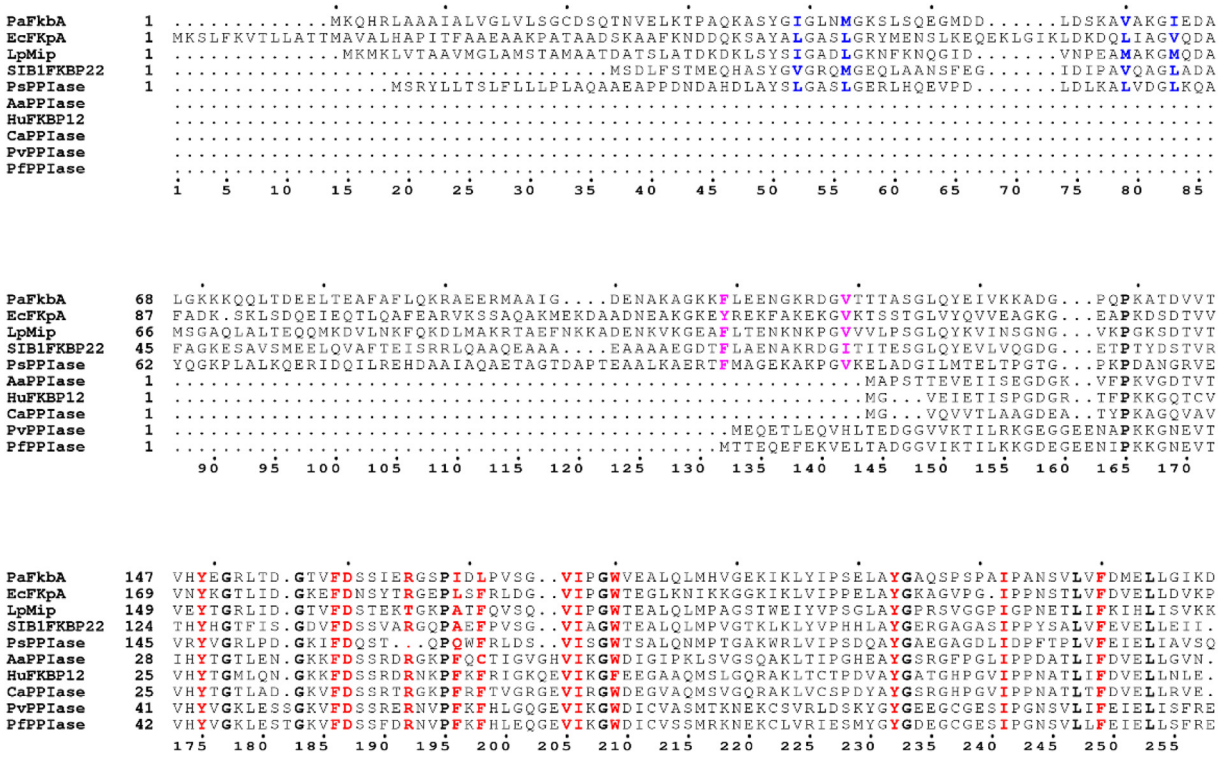

Fig. 3. Multiple Sequence alignment of PaFkbA-Δc and homologous Mip-like proteins from different organisms. Proteins are shown as *Legionella pneumophila* (LpMip, Uniprot code: Q5ZXE0), *Homo sapiens* (HuFKBP12, Uniprot code: P68106) and *Escherichia. coli* (EcFkpA, Uniprot code: P45523), *Pseudomonas syringae* pv. Tomato (PsPPIase, Uniprot code: Q88B84), *Aedes aegypti* (AaPPIase, Uniprot code: Q1HR83), *Candida auris* (CaPPIase, Uniprot code: A0A2H1A4Z6), *Plasmodium vivax* (PvPPIase, Uniprot code: A5K8X6), *Plasmodium falciparum* (PfPPIase, Uniprot code: Q8I4V8), *Shewanella* sp. SIB1 (SIB1PPIase, Uniprot code: Q765B0). Conserved "zipper knot" residues (blue), hydrophobic residues in FK506 binding cavity (red) and hinge helix that mediate interaction with FKBP domain (purple) are colored respectively. Other conserved residues are shown in bold format. (For interpretation of the references to colour in this figure legend, the reader is referred to the web version of this article.)

a switching module to tether the long helix in specific conformations.

3.5. Probe the structural characteristics important for PaFkbA chaperone activity

To evaluate the significance of the structural features of PaFkbA, we introduced multiple site-directed mutations at N-terminus (N42, K45, Q73, D77, E78), hinge region (D53, D54, R90, R94) and C-terminus (I177, Y203), and purified FKBP domain' truncated version (PaFkbA-Δ_{FKBP}). These purified samples were folded and subjected to the MucD refolding assay (Figure A4). As anticipated, all mutants showed remarkably reduced chaperone activity for MucD (Fig. 6). Notably, PaFkbA-Δ_{FKBP} did not exhibit any refolding effect on MucD. It suggested the indispensable role of the FKBP domain of MucD folding in contrast with EcFkpA. Based on previous studies

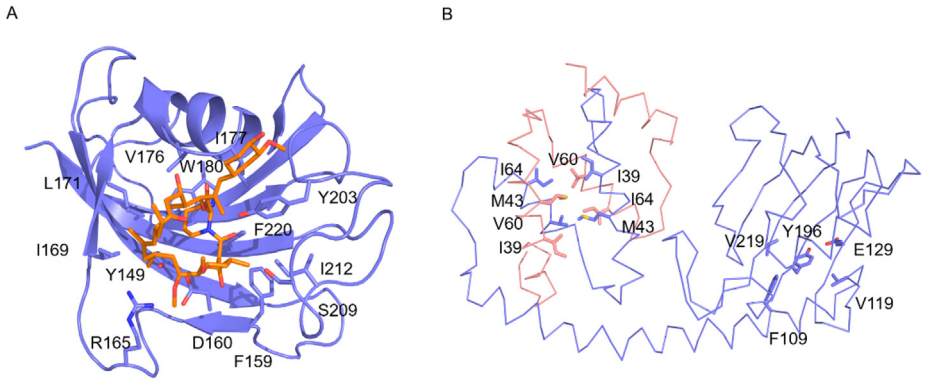

Fig. 4. Model of FK506-binding complex and structural distribution of critical sites for interdomain interaction. A. The modeled hydrophobic pocket of PaFkbA-Δc and interaction details between FKBP domain (blue) and peptide substrate FK506 (orange) are shown in sticks and labeled. B. Important residues for domain dimerization and interdomain interactions between FKBP domain and hinge region are displayed in sticks. (For interpretation of the references to colour in this figure legend, the reader is referred to the web version of this article.)

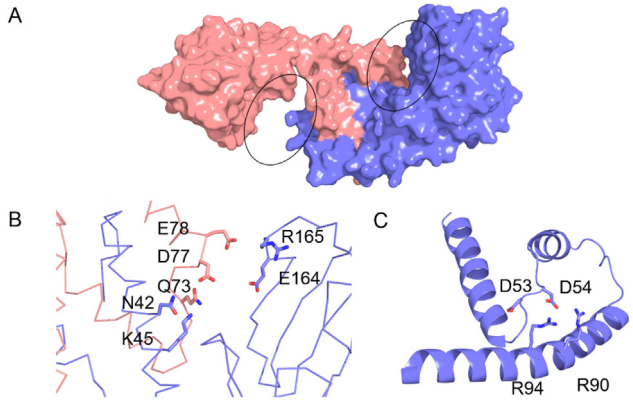

Fig. 5. Hinge in the connecting α3-helix controls domain motions. A. Effect of hinge region in inter-domain flexibility. The distance between FKBP domain and dimerization domain varies over time, allowing a wider cleft to bind to target molecules. B. Essential residues involved in forming a narrower cleft, which indicates a "close" state. C. Critical residues contribute to the flexibility of hinge helix are shown.

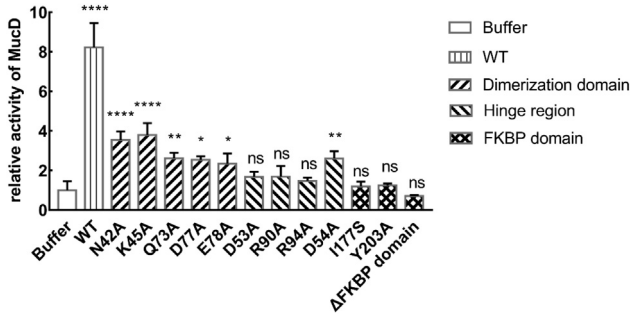

Fig. 6. Enzyme activity of refolded MucD in presence of PaFkbA-Δc mutants. The enzymatic experiment of refolded MucD by PaFkbA-Δc (WT, vertical bar) was performed as previously, while eleven mutants in dimerization domain (slash), hinge region (backslah) and a truncation of FKBP domain (grid line) were introduced and compared with control group (blank). Error bars represent the standard deviation of three duplicate trials. Statistical significance was calculated by one-way ANOVA (*, P < 0.05; **, P < 0.01; ****, P < 0.0001; ns, not significant).

on EcFkpA and LpMip [17,50], we constructed multiple PPIase function mutants by replacing the key active hydrophobic sites I177 and Y203 with Ser or Ala, respectively. These two PaFkbA variants also failed to promote the MucD folding in solution. Previous studies have shown that chaperone-like activity of Mip-like FKBPs is mainly associated with the N-terminal domain [17,21]. The FKBP domain truncated EcFkpA could catalyze the MalE31 or citrate synthase folding. Thus, the dependence of the FKBP domain and probably its PPIase activity on PaFkbA-MucD association reflects a possible specific recognition mechanism of PaFkbA.

PaFkbA' closed conformation indicated that charge patches distributed over the inner surface of the V-cleft region might be necessary for inter-domain coupling. Consequently, when Ala substitutions were introduced at the corresponding charge residues (N42, K45, Q73, D77, and E78), the chaperone activity decreased by 3.1 to 5.5-folds. These findings validated the importance of these sites in PaFkbA function and implicated that the N-terminal domain and FKBP domain coordinate to execute the function of the substrate-loading clamp.

The intrinsic dynamic domain arrangements of the MIP proteins, including the rocking and wobbling motions of the α3, were visualized by comparing the open and closed states of PaFkbA (Fig. 5A). However, displacements of this large domain did not require disruption of the hinge helix structure. It indicated a rigid orientation of the connecting α3. Thus, the complementary charge-based interactions around the α3 hinge could be one of the mechanisms to withstand the bending deformations. A decrease in these local contacts could affect the inter-domain mobility, impairing the PaFkbA function, which was evident in the chaperone activity assay of this study, where point mutations altering the charge residues within the functional hinge region remarkably reduced or even abrogated its chaperone activity. Taken together, the structural and biochemical results demonstrated the indispensable roles of both N-terminal and FKBP domains and suggested the functional importance of the potential core hinge residues at α3.

4. Discussion

In this work, we demonstrated the crystal structure of FKBP-type PaFkbA-Δc from *P. aeruginosa.* The overall structure of PaFkbA-Δc could be categorized into three parts, identical to other members of the MIP-like family. Moreover, our in vitro observations provided evidence for the role of PaFkbA in MucD folding. We were intrigued by the correlation between the PaFkbA's chaperone activity and its structure. Our structural analysis, together with key residues mutants and domain truncation constructs, furthered our understanding of PaFkbA's structural characteristic and PaFkbA mediated protein refolding.

We observed that conformational change in PaFkbA may be required for target protein binding. A previous study revealed that the dynamic hinge motion in LpMip permitted the FKBP domain movement, which affected its ability to bind to its substrates [23].

Mother's arms model representing the relevance of hinge bending with its chaperone activities in EcFkpA was proposed in the previous report [26]. In PaFkbA-Δc structure, two forms of the hinge region, i.e., bending and stretching states, were presented simultaneously. It allowed us to exploit the interdomain movement for PaFkbA. Structural analysis of PaFkbA and mutagenesis data revealed the hinge domain's role, which defined the protein conformation. Disrupting the local structure of the hinge region sharply reduced the PaFkbA' chaperone activity. This finding validated the importance of the hinge region in the PaFkbA function. We proposed a basic hypothesis based on the proximity of the N-terminus residues and the hydrophobic pocket of the C-terminus in the closed PaFkbA structure. We hypothesized that these two parts could form a cleft for substrate binding. The outcomes of our analysis demonstrated that PaFkbA chaperon activity for MucD folding depends on the PPIase and the N-terminal domains.

Most bacteria contain a complex stress response mechanism to deal with adverse environmental conditions. Molecular chaperones are the central components of bacterial stress responses and serve as direct virulence factors in multiple pathogens [17,51]. Without providing any energy input to the cellular periplasm, gram-negative bacteria employ multiple specialized chaperones to assist the protein folding and stabilization. EcFkpA and DegP are multi-function periplasmic chaperones that are involved in the sigma E pathway in *E. coli*. These chaperones have been suggested to perform a general periplasmic folding function, particularly under heat shock conditions. These chaperons might substitute each other, or they are required for the survival of bacteria under specialized circumstances. Previous studies have addressed their overlapping roles and physiological significance in bacterial adhesion, motility, biofilm formation, and virulence and implicated their crosstalk and connection during bacterial infections [17,18,52]. EcFkpA and DegP orthologs (PaFkbA and MucD) in *P. aeruginosa* were found to be associated with bacterial adaptation in host niches[30]. In this study, for the first time, we proved the chaperone activity of PaFkbA for MucD folding; besides, we biochemically demonstrated the direct correlation between these two chaperones. Chaperone activity of Mip-type PPIase was found to be distinct from the FKBP domain-independent chaperone activity [21]. PaFkbA chaperone function for MucD required the context of the whole protein, and it was found to be highly sensitive to mutations in both the N-terminal and C-terminal domains. These observations provided evidence for the PaFkbA-MucD coupling. The indispensable role of the additional domain for chaperone activity has been reported in many other multidomain PPIases such as trigger factor, a ribosome-associated PPIase [53]. However, its chaperone-like activity and its efficient folding activity for unfolded proteins required both FKPB and accessory domains. The interplay between PaFkbA and MucD suggests a coordinated function of multiple periplasmic chaperones. Nevertheless, the contribution of the PPIase activity of PaFkbA for MucD protein folding still needs additional evaluation. More research investigation and guidance are required to discern the detailed biological aspects associated with the PaFkbA-MucD coupling.

Accession numbers

The atomic coordinates of the refined structures have been deposited in the Protein Data Bank (www.wwpdb.org) under the PDB code 7DEK [54].

Declaration of Competing Interest

The authors declare that they have no known competing financial interests or personal relationships that could have appeared to influence the work reported in this paper.

Acknowledgements

The work was financially supported by National Key Research and Development Program of China (Grant No. 2016YFA0502700, National Mega-project for Innovative Drugs (Grant No. 2019ZX09721001-001-001), National Natural Science Foundation of China (Grant No. 81871615, 81670008), Ministry of Science and Technology of the People's Republic of China (Grant No. 2018ZX09201018-005). We thank National Center for Protein Sciences Shanghai (NCPSS) beamlines BL18U and BL19U for beamtime allowance. We thank the staffs of National Center for Protein Sciences Shanghai (NCPSS) beamlines BL18U and BL19U and Shanghai Synchrotron Radiation Facility (SSRF) BL17U, Shanghai, People's Republic of China, for assistance during data collection. We thank NCBI (http://www.ncbi.nlm.nih.gov/) and UniProt Knowledgebase (https://www.uniprot.org/) for providing the genome sequences of *Pseudomonas aeruginosa* (strain ATCC 15692/PAO1).

Appendix A. Supplementary data

Supplementary data to this article can be found online at https://doi.org/10.1016/j.csbj.2021.04.045.

References

[1] M, J., et al., FKBP Ligands-Where We Are and Where to Go? Frontiers in pharmacology, 2018. 10.3389/fphar.2018.01425
[2] Schmidpeter, P.A.M. and F.X. Schmid, Prolyl Isomerization and Its Catalysis in Protein Folding and Protein Function. 2015. 427(7): p. 1609-1631
[3] Pemberton TJ. Identification and comparative analysis of sixteen fungal peptidyl-prolyl cis/trans isomerase repertoires. BMC Genomics 2006;7(1):244–74.
[4] Cianciotto NP, Eisenstein BI, Engleberg CHMC. A Mutation in the mip Gene Results in an Attenuation of *Legionella pneumophila* Virulence. J Infect Dis 1990;162(1):121–6.
[5] Cianciotto NP et al. A *Legionella pneumophila* gene encoding a species-specific surface protein potentiates initiation of intracellular infection. Infect Immun 1989;57(4):1255–62.
[6] Henderson and Brian, An overview of protein moonlighting in bacterial infection. Biochemical Society Transactions, 2014. 42(6): p. 1720-1727.
[7] Wagner, C., et al., Collagen binding protein Mip enables Legionella pneumophila to transmigrate through a barrier of NCI-H292 lung epithelial cells and extracellular matrix. 2007. 9(2): p. 450-462
[8] Debroy S et al. *Legionella pneumophila* Mip, a Surface-Exposed Peptidylproline cis-trans-Isomerase, Promotes the Presence of Phospholipase C-Like Activity in Culture Supernatants. Infect Immun 2006;74(9):5152.
[9] Rasch, et al., PPIases Mip and PpiB of Legionella pneumophila contribute to surface translocation, growth at suboptimal temperature and infection. Infection & Immunity, 2018. 87(1): p. e00939-17
[10] Mo Y, Cianciotto NP, Mallavia LP. Molecular cloning of a *Coxiella burnetii* gene encoding a macrophage infectivity potentiator (Mip) analogue. Microbiology 1995;141(Pt 11)(11):2861–71.
[11] Norville IH et al. A *Burkholderia pseudomallei* macrophage infectivity potentiator-like protein has rapamycin-inhibitable peptidylprolyl isomerase activity and pleiotropic effects on virulence. Infect Immun 2011;79(11):4299.
[12] Leuzzi R et al. Ng-MIP, a surface-exposed lipoprotein of *Neisseria gonorrhoeae*, has a peptidyl-prolyl cis/trans isomerase (PPIase) activity and is involved in persistence in macrophages. Mol Microbiol 2010;58(3):669–81.
[13] Rockey DD et al. A 28 kDa major immunogen of Chlamydia psittaci shares identity with Mip proteins of *Legionella* spp. and *Chlamydia trachomatis* - cloning and characterization of the *C. psittaci* mip-like gene. Microbiology 1996;142(Pt 4)(4):945–53.
[14] Moro A et al. Secretion by *Trypanosoma cruzi* of a peptidyl-prolyl cis-trans isomerase involved in cell infection. EMBO J 1995;14(11):2483–90.
[15] Debroy S et al. *Leishmania infantum chagasi*: A genome-based approach to identification of excreted/secreted proteins. Exp Parasitol 2010;126(4):582–91.
[16] Zang N et al. Requirement of a mip-like gene for virulence in the phytopathogenic bacterium *Xanthomonas campestris* pv. campestris. Molecular plant-microbe interactions. MPMI 2007;20(1):21.
[17] Jean-Philippe, et al., Chaperone function of FkpA, a heat shock prolyl isomerase, in the periplasm of Escherichia coli. Molecular Microbiology, 2001. 39(1): p. 199-210.
[18] Hullmann J et al. Periplasmic chaperone FkpA is essential for imported colicin M toxicity. Mol Microbiol 2010;69(4):926–37.

[19] Ruiz-Perez F, Henderson IR, Nataro JP. Interaction of FkpA, a peptidyl-prolyl cis/trans isomerase with EspP autotransporter protein. Gut Microbes 2010;1 (5):339–44.
[20] Riboldi-Tunnicliffe A et al. Crystal structure of Mip, a prolylisomerase from *Legionella pneumophila*. Nat Struct Biol 2001;8(9):779–83.
[21] Saul FA et al. Structural and functional studies of FkpA from *Escherichia coli*, a cis/trans peptidyl-prolyl isomerase with chaperone activity. J Mol Biol 2004;335(2):595–608.
[22] A., P. and R. K., High enzymatic activity and chaperone function are mechanistically related features of the dimeric Escherichia coli peptidyl-prolyl-isomerase FkpA. Journal of Molecular Biology, 2001. 310: p. 485-498.
[23] Horstmann M et al. Domain Motions of the Mip Protein from *Legionella pneumophila*. Biochemistry 2006;45(40):12303–11.
[24] Kohler R et al. Biochemical and Functional Analyses of the Mip Protein: Influence of the N-Terminal Half and of Peptidylprolyl Isomerase Activity on the Virulence of *Legionella pneumophila*. Infect Immun 2003;71(8):4389.
[25] Budiman C et al. Crystal structure of N-domain of FKBP22 from *Shewanella* sp. SIB1: dimer dissociation by disruption of Val-Leu knot. Protein Sci 2011;20 (10):1755–64.
[26] Hu K, Galius V, Pervushin K. Structural Plasticity of Peptidyl Prolyl Isomerase sFkpA Is a Key to Its Chaperone Function As Revealed by Solution NMR. Biochemistry 2006;45(39):11983–91.
[27] S., et al., Novel Inner Membrane Retention Signals in Pseudomonas aeruginosa Lipoproteins. Journal of Bacteriology, 2008. 190(18) : p. 6119-6125.
[28] Davide V et al. Analysis of *Pseudomonas aeruginosa* Cell Envelope Proteome by Capture of Surface-Exposed Proteins on Activated Magnetic Nanoparticles. PLoS ONE 2012;7(11):e51062.
[29] DongSic DK et al. Proteomic analysis of outer membrane vesicles derived from *Pseudomonas aeruginosa*. Proteomics 2011;11(16):3424–9.
[30] Sriramulu DD, Nimtz M, Romling U. Proteome analysis reveals adaptation of *Pseudomonas aeruginosa* to the cystic fibrosis lung environment. Proteomics 2010;5(14):3712–21.
[31] BOUCHER JC et al. Two distinct loci affecting conversion to mucoidy in *Pseudomonas aeruginosa* in cystic fibrosis encode homologs of the serine protease. HtrA. 1996.
[32] Otwinowski Z, Minor W. Processing of X-ray diffraction data collected in oscillation mode. Methods Enzymol 1997;276(10):307–26.
[33] McCoy AJ et al. Phaser crystallographic software. J Appl Crystallogr 2007;40(Pt 4):658–74.
[34] Emsley P et al. Features and development of Coot. Acta Crystallographica Section D 2010;66(4):486–501.
[35] Delano WL. The PyMol Molecular Graphics System. Proteins Struct Funct Bioinf 2002;30:442–54.
[36] Missiakas D, Raina S. Protein misfolding in the cell envelope of *Escherichia coli*: new signaling pathways. 1997;22(2):59–63.
[37] F., et al., Molecular chaperones in cellular protein folding. Current Opinion in Structural Biology, 1995. 11(9): p. e0162922.
[38] Hohfeld J, Cyr DM, Patterson C. From the cradle to the grave: molecular chaperones that may choose between folding and degradation. EMBO Rep 2001;2(10):885–90.
[39] Vertommen D et al. The disulphide isomerase DsbC cooperates with the oxidase DsbA in a DsbD-independent manner. Mol Microbiol 2010;67 (2):336–49.
[40] Esther B et al. DegP Chaperone Suppresses Toxic Inner Membrane Translocation Intermediates. PLoS ONE 2016;11(9):e0162922.
[41] Egler M et al. Role of the Extracytoplasmic Function Protein Family Sigma Factor RpoE in Metal Resistance of *Escherichia coli*. J Bacteriol 2005;187 (7):2297.
[42] Yorgey P et al. The roles of mucD and alginate in the virulence of *Pseudomonas aeruginosa* in plants, nematodes and mice. Mol Microbiol 2010;41(5):1063–76.
[43] Damron FH, Yu HD. *Pseudomonas aeruginosa* MucD regulates the alginate pathway through activation of MucA degradation via MucP proteolytic activity. J Bacteriol 2010;193(1):286–91.
[44] Ju Y et al. Discovery of Novel Peptidomimetic Boronate ClpP Inhibitors with Noncanonical Enzyme Mechanism as Potent Virulence Blockers in Vitro and in Vivo. J Med Chem 2020;63(6):3104–19.
[45] Hottenrott S et al. The *Escherichia coli* SlyD Is a Metal Ion-regulated Peptidyl-prolyl cis/trans-Isomerase - ScienceDirect. J Biol Chem 1997;272 (25):15697–701.
[46] Fumagalli U et al. FK506 binding protein from a thermophilic archaeon, *Methanococcus thermolithotrophicus*, has chaperone-like activity in vitro. Biochemistry 2000;39(2):453–62.
[47] Lücke, et al., Insights into Immunophilin Structure and Function. Current Medicinal Chemistry, 2011. 18(35): p. 5333-5354.
[48] Schiene-Fischer and Cordelia, Multidomain Peptidyl Prolyl cis/trans Isomerases. Biochimica et Biophysica Acta. General Subjects, 2015. 1850(10): p. 2005-2016.
[49] Barik and Sailen, Bioinformatic Analysis Reveals Conservation of Intrinsic Disorder in the Linker Sequences of Prokaryotic Dual-family Immunophilin Chaperones. Computational and Structural Biotechnology Journal, 2017: p. S2001037017300971.
[50] Ludwig B et al. Characterization of Mip proteins of *Legionella pneumophila*. FEMS Microbiol Lett 1994;118(1–2):23–30.
[51] Lipinska B et al. Identification, characterization, and mapping of the *Escherichia coli* htrA gene, whose product is essential for bacterial growth only at elevated temperatures. 1989;171(3):1574–84.
[52] Skagia A et al. Cyclophilin PpiB is involved in motility and biofilm formation via its functional association with certain proteins. Genes Cells 2016;21 (8):833–51.
[53] Stoller G et al. A ribosome-associated peptidyl-prolyl cis/trans isomerase identified as the trigger factor. EMBO J 1995;14(20):4939–48.
[54] Berman, H., K. Henrick, and H. Nakamura, Berman, H, Henrick, K and Nakamura, H. Announcing the worldwide Protein Data Bank. Nat Struct Biol 10: 980. Nature Structural Biology, 2004. 10(12): p. 980.